Progress In Electromagnetics Research, Vol. 146, 99–108, 2014

An Independently Tunable Dual-Band Filter Using Asymmetric $\lambda/4$ Resonator Pairs with Shared Via-Hole Ground

Fei Liang*, Xiaofei Zhai, Wenzhong Lu, Qianxing Wan, and Yanyu Zhang

Abstract—This paper presents a dual-band tunable bandpass filter with independently controllable dual passbands based on a novel asymmetric $\lambda/4$ resonator pair with shared via-hole ground. Because two separated passbands can be independently generated by the two $\lambda/4$ resonators with different electric lengths, the asymmetric $\lambda/4$ resonator pair can realize flexible passband allocation when it is utilized to design dual-band filters. Two varactors are placed at the two open circuit ends of the asymmetric $\lambda/4$ resonator pair to control the two dominant resonant frequencies, respectively. A prototype tunable dual-band filter with Chebyshev response is designed and fabricated. The measured results are in good agreement with the full-wave simulated ones. The results show that the first passband varies in a frequency range from 0.88 GHz to 1.12 GHz with the 3-dB fractional bandwidth of 5.1%–6.4%, while the second passband can be tuned from 1.5 GHz to 1.81 GHz with the 3-dB fractional bandwidth of 5.4%–6.4%.

1. INTRODUCTION

In multiband wireless communication systems, multiband microwave components as fundamental parts are important. Especially, the multiband bandpass filters with tunable center frequency are getting more and more attention owing to their potential to meet the present requirements of system size and complexity.

In the past few years, a few methods are applied in the design of microstrip tunable dual-band filters [1–5]. Some tunable filters are implemented by RF-MEMS capacitors with low insertion loss and high Q at RF, but RF-MEMS capacitors are relatively expensive which blocks them from wide applications in microwave filter. Compared with RF-MEMS capacitors, varactor diodes have the advantage of higher reliability, lower cost and faster tuning speed, so they are widely used in the tunable microstrip filters [6–13]. An improved ring resonator loaded by two varactor diodes realized dual passbands [13]. In addition, varactor-loaded stepped-impedance resonators were used to design a tunable dual-band filter [14]. However, these reported tunable dual-band filters can only tune one of the dual passbands. Girdhari Chaudhary reported a tunable dual-band filter based on a pair of identical dual-mode resonators. However, the two passbands of this filter were highly affected by each other [15]. In [16], an independently controllable dual passbands filter with six varactor diodes and four dc biasing circuits was realized by utilizing a pair of different dual-mode resonators. However, its tuning steps were very complicated, and circuit size was also relatively large because it requires a large number of varactor diodes and biasing circuits.

In this paper, we propose a novel asymmetric $\lambda/4$ resonator pair with shared via-hole ground to realize dual-band response. Because two separated passbands are independently generated by the two

Received 25 March 2014, Accepted 17 April 2014, Scheduled 4 May 2014

* Corresponding author: Fei Liang (liangfei@mail.hust.edu.cn).

The authors are with the School of optical and electronic information, Huazhong University of Science and Technology, Wuhan 430074, P. R. China.

$\lambda/4$ resonators with different electric lengths, the asymmetric $\lambda/4$ resonator pair can realize flexible passband allocation. By designing appropriate coupled structure, each passband of dual-band filter can be tuned independently by tuning respectively varactor diodes placed at the two open circuit ends of the asymmetric $\lambda/4$ resonator pair. In the proposed structure, the filter requires a small number of varactor diodes, and its circuit structure is relatively simple. To provide an experimental validation on our proposed filters, a prototype tunable dual-band filter is designed, fabricated and measured.

2. THEORETICAL ANALYSIS OF PROPOSED CONCEPT

2.1. The Property of the Asymmetric $\lambda/4$ Resonator Pair

The basic structure of the proposed asymmetric $\lambda/4$ resonator pair with shared via-hole ground is shown in Figure 1(a) [18]. And the basic resonance theory of microstrip line is applied to discuss the resonant frequencies.

As shown in Figure 1(a), the proposed resonator pair is composed of two different resonators (A and B). W stands for the width of resonator A and decides the characteristic impedance of resonator A. L_1 and L_2 stand for the lengths of resonator A and B, respectively. D is the diameter of the via-hole.

Take resonator A for example, the input admittance of resonator A is given by:

$$Y_{in} = -jY_1 \cot(\beta L_1) \tag{1}$$

where β represents the phase constant of the transmission line and Y_1 the characteristic admittance of resonator A. The resonator should achieve zero input admittance under resonance, and by using resonant condition, the fundamental resonant frequency can be determined as follows:

$$L_1 = \frac{V_P}{4f_A} = \frac{c}{4f_A\sqrt{\varepsilon_{eff}}} \tag{2}$$

where c is the velocity of light in free space, ε_{eff} the effective permittivity of substrate, and f_A the fundamental resonant frequency of resonator A. It is observed that the fundamental resonant frequency of resonator A is determined by the length of microstrip transmission line in the case that the substrate is chosen firstly.

Figure 1(b) shows that the fundamental frequencies of resonators A and B vary with the value of L_2 while other parameters keep constant. According to Figure 1(b), the fundamental resonant frequency f_A is almost not affected by L_2, and the fundamental resonant frequency f_B varies with the value of L_2, because the frequencies f_A and f_B are independently generated by the two $\lambda/4$ resonators with different electric lengths L_1 and L_2, respectively. Thus, the above two resonant frequencies f_A and f_B can be used to design a novel tunable dual-band filter with two independently controllable passbands.

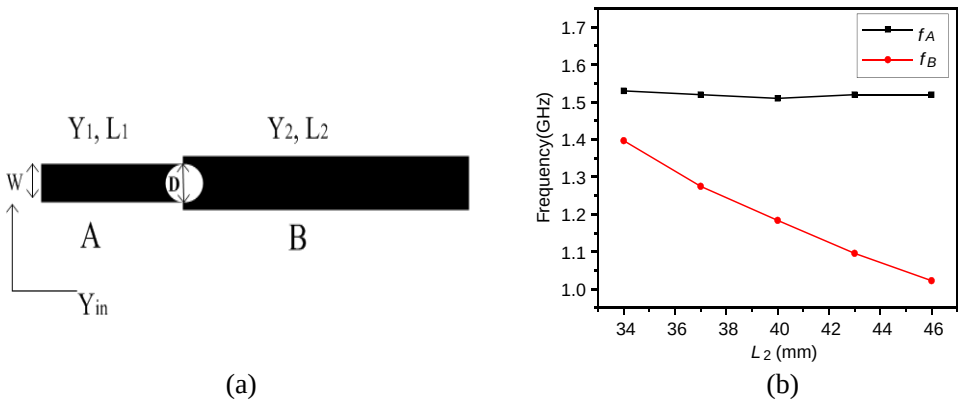

Figure 1. (a) Basic structure of the proposed asymmetric $\lambda/4$ resonator pair with shared via-hole ground. (b) Simulation of f_A and f_B varying with the value of L_2.

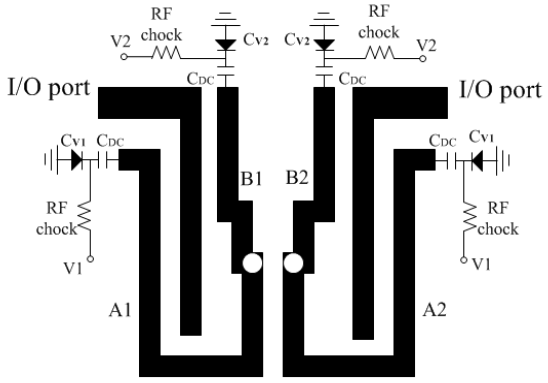

Figure 2. Layout of the proposed two-pole dual-band tunable filter.

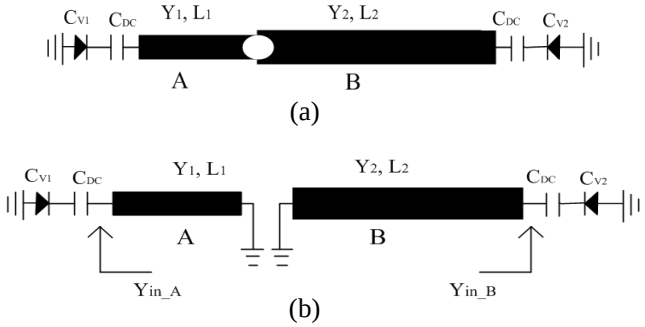

Figure 3. (a) Basic structure of the proposed resonator pair. (b) Equivalent circuit of basic structure.

2.2. Configuration of the Proposed Filter

Figure 2 shows the layout of the proposed tunable microstrip dual-band bandpass filter. It consists of two asymmetric $\lambda/4$ resonator pairs with common input and output ports. Resonators A1 and B1 are identical to resonators A2 and B2, respectively. Two varactor diodes are placed at the open circuit ends of the asymmetric $\lambda/4$ resonator pair. Resonators A1 and A2 simultaneously resonate at the first passband center frequency (f_A) while resonators B1 and B2 simultaneously resonate at the second passband center frequency (f_B).

2.3. Characteristics of Designed Resonator Loaded by Varactor Diodes

Figure 3 shows the structure of the proposed resonator pair with two varactor diodes (C_{V1} and C_{V2}) attached at the open circuit ends of the transmission line. And two different dc biasing circuits are used to provide bias voltages for two sets of varactor diodes in the structure, respectively. The dc block capacitor C_{DC} is between the ends of the microstrip line and the varactor diode. The parasitic effects of varactor diodes and the effects of microstrip line discontinuity are neglected in order to simplify analysis.

As shown in Figure 3(b), when the external RF signal is applied to the ends of the proposed resonators A and B, the input admittances are expressed as follows:

$$Y_{in\_A} = j\left[wC_{t1} - Y_1 \cot(\beta_1 L_1)\right] \tag{3}$$

$$Y_{in\_B} = j\left[wC_{t2} - Y_2 \cot\left(\beta_2 L_2\right)\right] \tag{4}$$

where C_t is the total capacitance for series connection of the varactor diode and dc block capacitor, which are given by [16]:

$$C_{t1} = \frac{C_{V1}C_{DC}}{C_{V1} + C_{DC}} \tag{5}$$

$$C_{t2} = \frac{C_{V2}C_{DC}}{C_{V2} + C_{DC}} \tag{6}$$

By using the resonance condition, the resulting resonant frequencies can be derived as:

$$2\pi C_{t1} f_A \tan\left(\frac{2\pi f_A L_1 \sqrt{\varepsilon_{eff}}}{c}\right) = Y_1 \tag{7}$$

$$2\pi C_{t2} f_B \tan\left(\frac{2\pi f_B L_2 \sqrt{\varepsilon_{eff}}}{c}\right) = Y_2 \tag{8}$$

Obviously, it can be observed that the resonant frequency is determined by transmission line L and total capacitance C_t from Equations (5)–(8). When C_{DC} and C_{V1} connected at the open circuit end

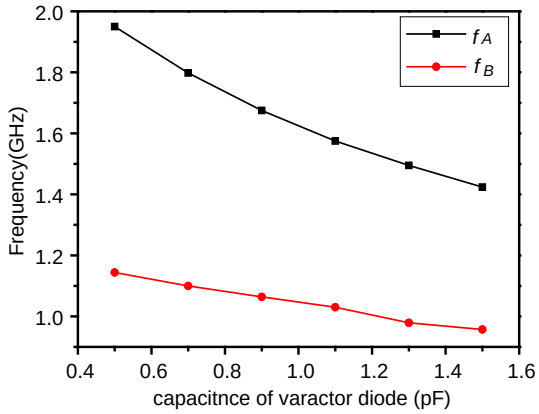

Figure 4. Tuning ranges of resonant frequencies. (The other dimension parameters: $Y_1 = 1.3\,\text{mm}$, $L_1 = 17.2\,\text{mm}$, $Y_2 = 1.9\,\text{mm}$, $L_2 = 39\,\text{mm}$).

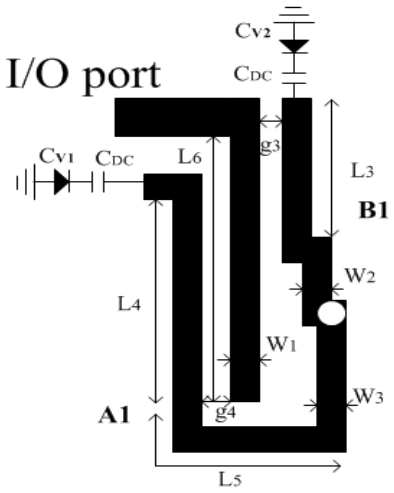

Figure 5. Circuit of Input/Output coupling scheme.

of the transmission line L_1 are fixed, it is pretty easy to understand that the resonant frequency f_A is fixed, and the resonant frequency f_B can be tuned only by changing C_{V2}. On the other hand, when C_{DC} and C_{V2} are fixed, the resonant frequency f_A can be tuned by changing C_{V1}, and the resonant frequency f_B is fixed. Moreover, as C_{V1} and C_{V2} vary at the same time, f_A and f_B can be tuned simultaneously and separately. So a band-pass filter with two independently controllable passbands can be designed by utilizing the above-mentioned characteristic of proposed resonator. Given the suitable fixed geometry dimensions, the variation ranges of two passbands with capacitance of varactor diodes changed from 0.5 to 1.5 pF are shown in Figure 4.

2.4. External Quality Factors

Since the structure of the proposed filter is symmetrical, the external quality factors can be discussed by the half circuit. Figure 5 shows the basic configuration of I/O coupling scheme.

The external quality factor related to Input/Output coupling strength can be determined by:

$$Q_{e1} = f_A/\Delta f_{A\pm 90^\circ} \tag{9}$$

$$Q_{e2} = f_B/\Delta f_{B\pm 90^\circ} \tag{10}$$

where $\Delta f_{A\pm 90^\circ}$ and $\Delta f_{B\pm 90^\circ}$ are the absolute bandwidths with phase shift $\pm 90^\circ$ at the resonant frequencies f_A and f_B, respectively.

To simplify the design, suitable capacitances of varactor diodes are chosen firstly. Then it is useful to use the full-wave electromagnetic simulation (Ansoft HFSS 13) to discuss the effects of structural parameters on the external quality factor. In [16], gap and coupling length between resonator and I/O lines dramatically affect external quality factors in the circuit, and the change rules of the desired external quality factors can be obtained from simulation results. Different g_3 and g_4 are simulated to investigate the change rules of external quality factors, with the other parameters fixed. As shown in Figure 6, Q_{e1} and Q_{e2}, which stand for the external quality factors at first and second passbands, increase with the increase of gaps.

The parameters (g_4, L_4, g_3, L_3, L_6) can be optimized by using these change rules to meet the requirement of the desired external quality factors Q_{e1} and Q_{e2} over the tuning ranges, respectively.

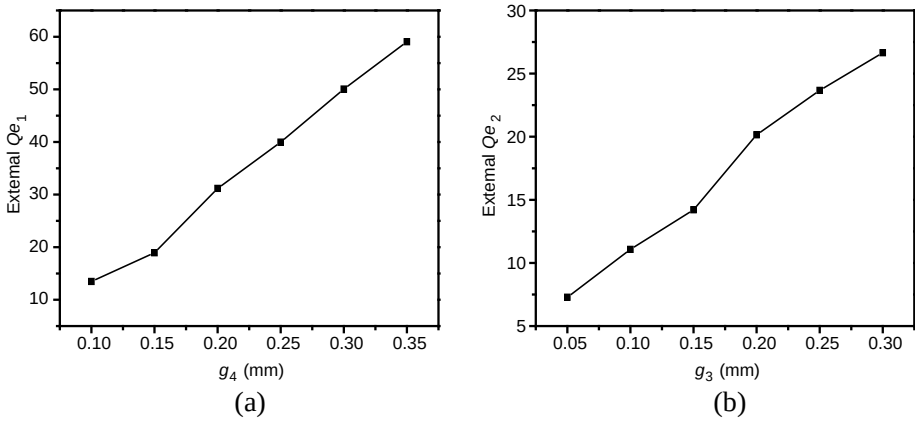

Figure 6. The external quality factors according to the gaps. (The other dimension parameters: $L_3 = 10\,\text{mm}$, $L_4 = 17\,\text{mm}$, $L_5 = 9.5\,\text{mm}$, $L_6 = 21\,\text{mm}$, $W_1 = 0.9\,\text{mm}$, $C_{DC} = 56\,\text{pF}$, $C_{V1} = 1.2\,\text{pF}$, $C_{V2} = 1.2\,\text{pF}$).

2.5. Coupling Coefficients (Ki)

The coupling coefficients of dual-band filter can control bandwidth of the two passbands. In order to verify the relationship between couplings coefficient of resonators and structure parameters, a coupling circuit is also designed and simulated by the software Ansoft HFSS 13, as shown in Figure 7.

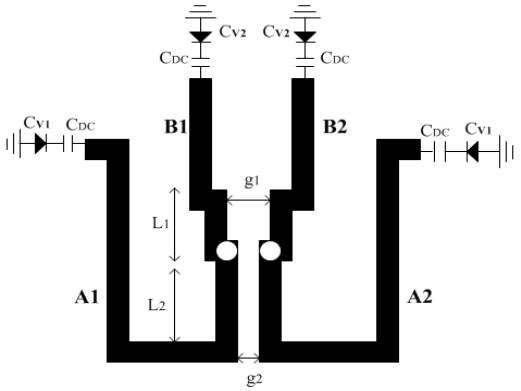

Figure 7. Circuit model of coupling coefficient.

In [15], the coupling coefficients (K_1 and K_2) controlled by gap and coupling length between the resonators of first and second passbands can be calculated as follows:

$$K_1 = \frac{f_{A1}^2 - f_{A2}^2}{f_{A1}^2 + f_{A2}^2} \tag{11}$$

$$K_2 = \frac{f_{B1}^2 - f_{B2}^2}{f_{B1}^2 + f_{B2}^2} \tag{12}$$

where f_{A1} and f_{A2}, f_{B1}, f_{B2} are the coupling separated mode resonant frequencies of f_A and f_B. In the case of the fixed load capacitor values, the dimension parameters are optimized separately to estimate the corresponding coupling coefficients. The estimated coupling coefficients as a function of gaps are shown in Figure 8. From the result, the coupling coefficients decrease as gaps increase.

Moreover, there is also basically no interference between the two coupling coefficients (K_1 and K_2) in the simulation process. By properly optimizing these parameters (g_2, L_2, g_1, L_1), the desired coupling coefficients and bandwidth of the two passbands can be gained.

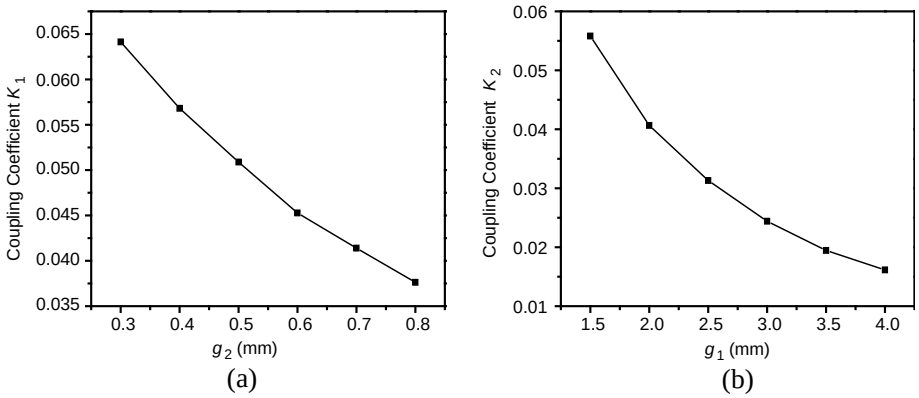

Figure 8. The external quality factors according to the gaps. (The other dimension parameters: $L_1 = 6.65\,\text{mm}$, $L_2 = 8.15\,\text{mm}$, $C_{DC} = 56\,\text{pF}$, $C_{V1} = 1.2\,\text{pF}$, $C_{V2} = 1.2\,\text{pF}$).

3. FILTER DESIGN AND MEASURED RESULTS

3.1. Design Index of Filter

To demonstrate the proposed idea, this work utilizes dc biasing circuits and varactor diodes to design a microstrip tunable dual-band filter of the following specifications:

- first tuning passband: 0.88–1.2 GHz;
- 3-dB FBW of first passband: 5.0%–6.5%;
- second tuning passband: 1.5–1.8 GHz;
- 3-dB FBW of second passband: 5.0%–6.5%;
- number of poles: two;
- type: Chebyshev frequency response.

3.2. Filter Design Procedure

A similar design procedure presented in [16, 17] is applied to design the proposed dual-band tunable BPF. The dimension parameters in Figure 2 can be determined as follows.

Step 1) Determine the dimensions of resonator to realize the tuning ranges of the two passbands: Firstly, the characteristic impedance of resonators can be designed as $70\,\Omega$ for convenience, and the electrical length of resonators and varactor should be carefully selected according to Equations (7) and (8). The capacitance variation range of varactor is particularly important because it directly decides frequency tuning range when physical length of the resonator is fixed. Moreover, it is difficult to make accurate calculations of parasitic parameters, e.g., resistors, inductors, etc. of the varactor in reality. Parasitic parameters almost keep constant with the change of voltage, and they make no contribution to the filter's tunability. So the parasitic parameters are neglected in this work.

Step 2) Determine the external quality factors and coupling coefficient: Select the second-order low-pass prototype and element value g_i, based on design index of the filter. And original values of the external quality factors and coupling coefficients can be gained as follow:

$$Q_e = \frac{g_0 g_1}{\text{FBW}} \tag{13}$$

$$K = \frac{\text{FBW}}{\sqrt{g_1 g_2}} \tag{14}$$

where FBW is the 3-dB fractional bandwidth of the passband, and g_0, g_1 and g_2 are the element values of the prototype low-pass filter.

Step 3) Determine the dimensions of coupling and input/output structures: according to Sections 2.4 and 2.5, the coupled lengths and gap widths greatly influence the above external quality

factors and coupling coefficients, and they should be suitably chosen to realize the required values of external quality factors and coupling coefficients. Moreover, relying on the change rules between the frequency response and dimension parameters obtained from full-wave simulation tool (Ansoft HFSS 13), dimension parameters should be continuously optimized until the design index of filter is fulfilled. Because there may be unexpected weak parasitic effects in measured results, circuit parameters will be fine-tuned to achieve the optimal resonant response.

3.3. Filter Implementation and Experimental Demonstration

After the final optimization, the dimension parameters and component values of the filter are listed as shown in Table 1. Figure 2 shows the ultimate layout of the designed tunable dual-band filter. To verify the simulation and above design theory basing on the asymmetric $\lambda/4$ resonator pair with shared via-hole ground, a compact tunable dual-band filter is fabricated on the substrate which is Rogers 4350B with the thickness of 0.762 mm, a dielectric constant of 3.5 and a loss tangent of 0.004. In the configuration, the input/output ports feeding the proposed resonators utilize two microstrip lines with characteristic impedance fixed at 50 Ω. Four capacitors functioning as dc blocking are RF chip capacitors from ATC Corporation, and a 500 nH inductance chip and a 10 Ohm resistance are connected in series in the dc biasing circuit, functioning as the reducing RF-signal leakage networks.

Four varactor diodes employed at the ends of resonators are SMV1405-079 from Skyworks Corporation, and the capacitance of single varactor diode varies from 2.67 to 0.63 pF with the value of bias voltage varying from 0 to 30 V. Because the capacitance variation of varactor diode with the bias voltage is not linear, the filter's tunability is not linear too. In addition, two passbands will be tuned in lager frequency ranges if varactor diodes with a larger range of capacitance are utilized, respectively.

A photograph of the fabricated filter is given in Figure 9, and the measurement is carried out by using Agilent Vector network analyzer E8362.

Figure 10 exhibits the simulated and measured results concerning the fixed first passband and controllable second passband. As depicted by Figure 10, the first passband frequency is fixed at 1.11 GHz with a insertion loss of 1.7 dB and 3-dB FBW of 6.3% under the constant bias voltage V_1. In the meantime, the second passband is controlled, the center frequency continuously tuned from 1.5 to 1.81 GHz with the value of bias voltage V_2 varying from 6 to 26 V, and the insertion loss is from 3.11 to 3.90 dB. Moreover, it is found that the second passband 3-dB FBW varies in the range of 5.4%–6.4%. The reasons for the above phenomenon can be that the coupling strength of electric and magnetic fields of the fabricated filter has some minor variations with the change of frequency. The return loss of the second passband is better than 13 dB, as shown in Figure 10(a).

Table 1. Dimensions of fabricated the filter (dimensions are in millimeters).

$L_1/L_2/L_3/L_4/L_5/L_6$	$W_1/W_2/W_3$	$g_1/g_2/g_3/g_4$	C_{DC} (pf)
6.6/8.1/10.5/17.5/9.5/21	0.9/1.3/1.9	2.4/0.6/0.2/0.2	56

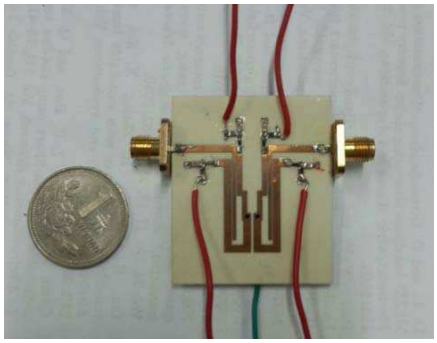

Figure 9. Fabricated tunable dual-band filter.

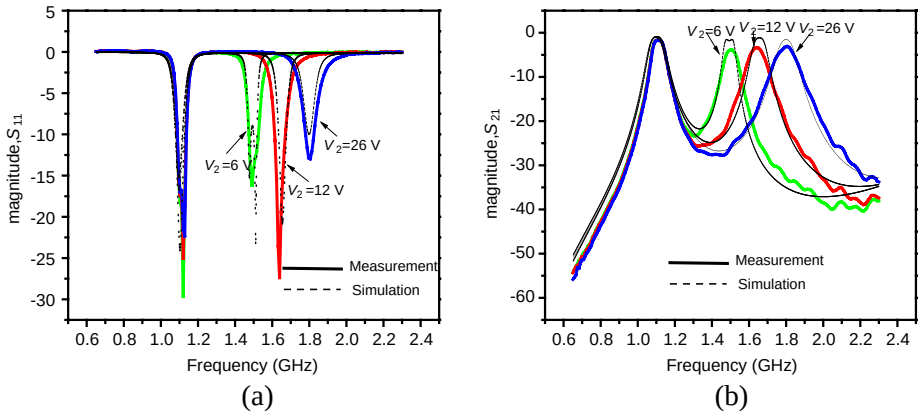

Figure 10. The simulated and measured results of the proposed filter with fixed first passband and tunable second passband. (a) S_{11}. (b) S_{21}. Bias voltage variation: $V_1 = 22\,\text{V}$ and $V_2 = 6\,\text{V}{\sim}26\,\text{V}$.

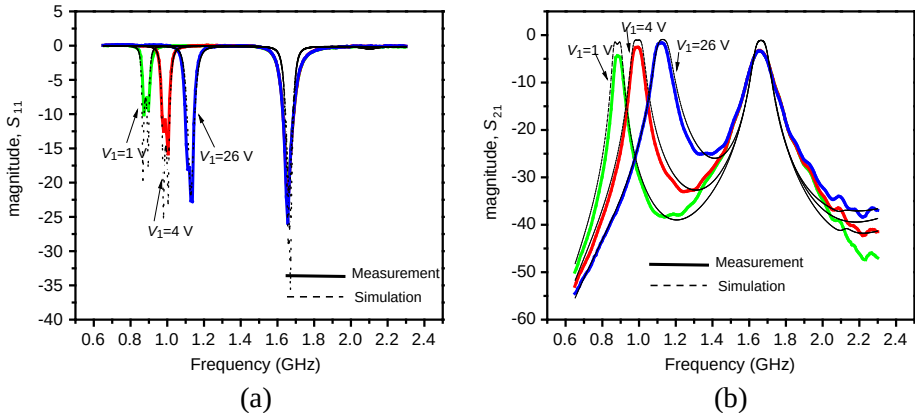

Figure 11. The simulated and measured results of the proposed filter with tunable first passband and fixed second passband. (a) S_{11}. (b) S_{21}. Bias voltage variation: $V_1 = 1\,\text{V}{\sim}26\,\text{V}$ and $V_2 = 13\,\text{V}$.

Figure 11 exhibits the simulated and measured results concerning the fixed second passband and controllable first passband. From Figure 11, the second passband center frequency is absolutely fixed at 1.66 GHz with insertion loss of 3.3 dB and 3-dB FBW of 6.0% under the constant bias voltage V_2. In the meantime, the first passband is controlled, the center frequency continuously tuned from 0.88 to 1.12 GHz with the value of bias voltage V_1 varying from 1 to 26 V, and the insertion loss is from 1.65 to 4.3 dB. Moreover, it is also found that the first passband 3-dB FBW varies in the range of 5.1%–6.4%. The return loss of the first passband is better than 10 dB, as shown in Figure 11(a).

Figure 12 exhibits the simulated and measured results of the fabricated filter by changing the values of two sets of bias voltages at the same time. As shown in Figure 12, the two passbands are not affected by each other at all, and can be tuned simultaneously and very conveniently. The first passband frequency can be tuned from 0.88 to 1.12 GHz with V_1 varying from 1 to 26 V, and the second passband frequency can be tuned from 1.5 to 1.81 GHz with V_2 varying from 6 to 26 V, respectively. And the insertion loss of the stopband between the two passbands is better than 25 dB.

In the overall tuning range, it is seen that the measurement results are consistent with the simulated ones. But the measured insertion loss is a little worse than the corresponding simulated one, which may result from the assembly machining errors and parasitic parameters of the varactor diodes [9]. In addition, Figure 12 shows that the two passbands have different tuning capabilities with the same varactors, due to the $\lambda/4$ resonators A and B with different characteristic admittances Y and electrical lengths L, respectively. According to Equations (7) and (8), the characteristic admittance Y and

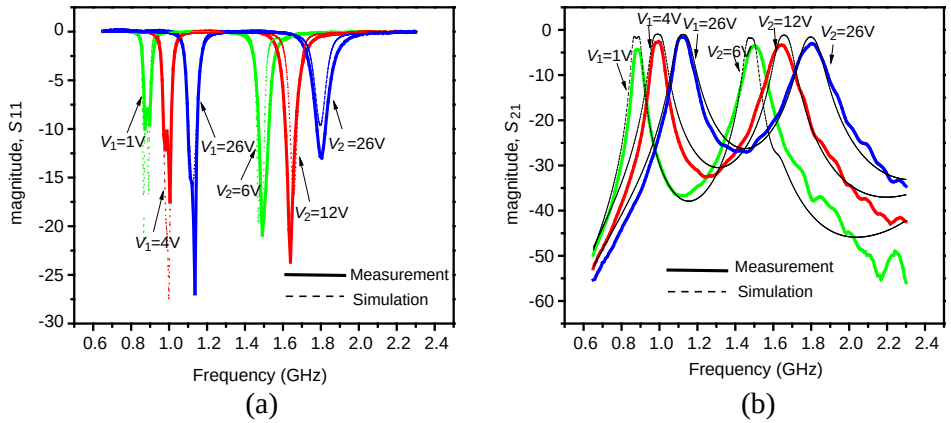

Figure 12. The simulated and measured results of the proposed filter with tunable first passband and second passband. (a) S_{11}. (b) S_{21}. Bias voltage variation: $V_1 = 1\,\text{V}\sim26\,\text{V}$ and $V_2 = 6\sim26\,\text{V}$.

Table 2. Comparison for tunable dual-band filters.

	1st Passband		2nd Passband		Types of bias circuits	Size (mm)	Lumped elements	A
	Frequency (GHz)	Insertion Loss (dB)	Frequency (GHz)	Insertion Loss (dB)				
[15]	0.85–1.2	0.85–2.42	1.4–2.14	1.2–3.3	2	$51 * 54$	Diode: 6 C_{DC}: 4	No
[16]	1.48–1.8	1.99–4.4	2.4–2.88	1.6–4.2	4	$27 * 40$	Diode: 6 C_{DC}: 6	Yes
[17]	0.77–1.02	0.7–1.4	1.57–2.0	2.74–3.93	2	$37 * 24$	Diode: 6 C_{DC}: 10	Yes
This work	0.88–1.12	1.65–4.3	1.5–1.81	3.11–3.9	2	$37 * 38$	Diode: 4 C_{DC}: 4	Yes

A = independently tunable two passbands.

electrical length L of the $\lambda/4$ resonator, especially the electrical length L, decide the frequency tuning range in the condition of the same capacitance variation. The shorter the electrical length L of the $\lambda/4$ resonator is, the wider the frequency tuning range in the condition of the same capacitance variation is. Table 2 shows performance comparisons between this paper and other recently published papers in the references.

Compared with other recently reported filters, two passbands of the filter in this work can be tuned independently and conveniently by only two types of dc biasing circuits. Moreover, it has an excellent performance and simpler resonant coupling topology with less lumped elements (varactor diodes and dc blocking capacitances). Therefore, design and manufacturing procedures are simpler.

4. CONCLUSION

In this paper, a novel tunable dual-band bandpass filter is investigated and fabricated by using proposed asymmetric $\lambda/4$ resonator pair with shared via-hole ground to achieve frequency tunability in the two passbands. According to the design equations and procedures, the novel proposed filter can realize two independently controllable passbands with small size and insertion loss, convenient tuning and manufacture for small numbers of control voltages and lumped elements. With these advantages, this type of filter can be widely used in the RF front circuits of mobile communication devices.

REFERENCES

1. Chen, J.-X., J. Shi, Z.-H. Bao, and Q. Xue, "Tunable and switchable bandpass filters using slot-line resonators," *Progress In Electromagnetics Research*, Vol. 111, 25–41, 2011.
2. Li, Z., X.-H. Wang, Z.-D. Wang, and Y.-F. Bai, "Compact electronically tunable microstrip dual-band filter using stub-loaded SIRs," *Journal of Electromagnetic Waves and Applications*, Vol. 28, No. 1, 39–48, 2014.
3. Zhang, X.-Y. and Q. Xue, "Novel centrally loaded resonators and their applications to bandpass filters," *IEEE Transactions on Microwave Theory and Techniques*, Vol. 56, No. 4, 913–921, 2008.
4. Girbau, D., A. Lazaro, E. Martinez, D. Masone, and L. Pardell, "Tunable dual-band bandpass filter for WLAN applications," *Microwave and Optical Technology Letters*, Vol. 51, 2025–2028, 2009.
5. Djoumessi, E. E., M. Chaker, and K. Wu, "Varactor-tuned quarter-wavelength dual-bandpass filter," *IET Microwaves, Antennas & Propagation*, Vol. 3, No. 1, 117–124, 2009.
6. Feng, T., Y. Li, H. Jiang, W. Li, F. Yang, X. Dong, and H. Chen, "Tunable single-negative metamaterials based on microstrip transmission line with varactor diodes loading," *Progress In Electromagnetics Research*, Vol. 120, 35–50, 2011.
7. Serrano, A. L. C., F. S. Correra, T.-P. Vuong, and P. Ferrari, "Synthesis methodology applied to a tunable patch filter with independent frequency and bandwidth control," *IEEE Transactions on Microwave Theory and Techniques*, Vol. 60, No. 3, 484–493, 2007.
8. Liu, B., F. Wei, and Q.-Y. Wu, "A tunable bandpass filter with constant absolute bandwidth," *Journal of Electromagnetic Waves and Applications*, Vol. 25, Nos. 11–12, 1596–1604, 2011.
9. Zhu, Y., R.-W. Mao, and S. T. Chen, "A varactor and FMR-tuned wideband band-pass filter module with versatile frequency tunability," *IEEE Transactions on Magnetics*, Vol. 47, No. 2, 284–288, 2011.
10. Wang, Y.-Y., F. Wei, H. Xu, and X. W. Shi, "A tunable 1.4-2.5 GHz bandpass filter based on single mode," *Progress In Electromagnetics Research*, Vol. 135, 261–269, 2013.
11. Liu, B., F. Wei, H. Zhang, and X. Shi, "A tunable bandpass filter with switchable bandwidth," *Journal of Electromagnetic Waves and Applications*, Vol. 25, Nos. 2–3, 223–232, 2011.
12. Zhang, H.-L., X. Y. Zhang, and B.-J. Hu, "Tunable bandpass filters with constant absolute bandwidth," *Antennas Propagation and EM Theory (ISAPE)*, 1200–1203, 2010.
13. Wu, Z.-H., F. Wei, and Y.-Y. Wang, "A tunable dual-passband filter based on improved ring resonator," *Journal of Electromagnetic Waves and Applications*, Vol. 24, No. 1, 141–149, 2010.
14. Wang, X.-H., L. Zhang, Y.-F. Bai, Y. Xu, and H. Xu, "Compact tunable dual-band filter using SIRs without extra blocking capacitances," *Journal of Electromagnetic Waves and Applications*, Vol. 27, No. 5, 544–551, 2013.
15. Chaudhary, G., J. Yongchae, and L. Jongsik, "Harmonic suppressed dual-band bandpass filters with tunable passbands," *IEEE Transactions on Microwave Theory and Techniques*, Vol. 60, No. 7, 2115–2123, 2012.
16. Chaudhary, G., J. Yongchae, and L. Jongsik, "Dual-band bandpass filter with independently tunable center frequencies and bandwidths," *IEEE Transactions on Microwave Theory and Techniques*, Vol. 61, No. 1, 107–116, 2013.
17. Huang, X.-G., L. Zhu, and Q.-Y. Feng, "Tunable bandpass filter with independently controllable dual passbands," *IEEE Transactions on Microwave Theory and Techniques*, Vol. 61, No. 9, 3200–3208, 2013.
18. Liang, F., B. Luo, W.-Z. Lu, and X.-C. Wang, "A compact dual-band filter with close passbands using asymmetric $\lambda/4$ resonator pairs with shared via-hole ground," *Journal of Electromagnetic Waves and Applications*, Vol. 25, Nos. 8–9, 1289–1296, 2011.